Thermochimica Acta 476 (2008) 44–50

Contents lists available at ScienceDirect

Thermochimica Acta

journal homepage: www.elsevier.com/locate/tca

Kinetic analysis of the non-isothermal degradation of poly(3-hydroxybutyrate) nanocomposites

Matko Erceg*, Tonka Kovačić, Sanja Perinović

Department of Organic Technology, Faculty of Chemistry and Technology, University of Split, Teslina 10/V, 21000 Split, Croatia

ARTICLE INFO

Article history:
Received 1 February 2008
Received in revised form 14 July 2008
Accepted 27 July 2008
Available online 5 August 2008

Keywords:
Kinetic analysis
Nanocomposites
Organoclay
Poly(3-hydroxybutyrate)
Non-isothermal thermogravimetry

ABSTRACT

Poly(3-hydroxybutyrate)/organically modified montmorillonite nanocomposites (PHB/25A) were prepared by the solution-intercalation method. The non-isothermal degradation of pure PHB and PHB/25A nanocomposites was investigated in the temperature range 50–500 °C at four heating rates (2.5, 5, 10 and 20 °C min^{-1}). Kinetic analysis of the non-isothermal degradation of pure PHB and PHB/25A nanocomposites was performed using isoconversional (Flynn-Wall-Ozawa, Kissinger-Akahira-Sunose and Friedman) methods and the invariant kinetic parameters method. The true kinetic triplets (E, A, and $f(\alpha)$) were determined.

1. Introduction

Poly(3-hydroxybutyrate) (PHB) is an aliphatic polyester obtained by bacterial fermentation. PHB is fully biodegradable, thermoplastic and it has some physical and mechanical properties, like tensile strength and Young's modulus [1–3], comparable to those of isotactic polypropylene [4–6]. PHB has several drawbacks, such as pronounced stiffness and brittleness due to high crystallinity and secondary crystallization, very low resistance to thermal degradation at processing temperatures. To improve these properties, we have prepared PHB nanocomposites with organically modified montmorillonite (Cloisite25A) as nanofiller [7].

In this work, kinetic analysis of the non-isothermal degradation of pure PHB and PHB nanocomposites with Cloisite25A was performed. To our knowledge, only few articles have been published concerning the kinetic analysis of the non-isothermal degradation of PHB and PHB based materials [8–10]. There are no articles concerning the kinetic analysis of the non-isothermal degradation of PHB nanocomposites at all. The activation energy (E) of the non-isothermal degradation of PHB was determined by various methods: Flynn-Wall-Ozawa and Kissinger [8], Horowitz–Metzger [9] and Coats-Redfern [10] methods. The reported values are inconsistent and they vary from 80 kJ mol^{-1} [8] to around 300 kJ mol^{-1} [9,10]. The values of the pre-exponential factor (A) are calculated by Coats-Redfern method under the assumption of the nth order reaction [10]. Coats-Redfern method is a model fitting method which uses single $\alpha - T$ data, obtained at a certain heating rate for the determination of the kinetic parameters. The use of methods that use single $\alpha - T$ data for the determination of the kinetic parameters should be avoided [11,12] because they generally cannot distinguish true from false kinetic model and tend to produce highly uncertain values of E and A.

These drawbacks of model fitting methods can be avoided by using isoconversional (model-free) methods which require $\alpha - T$ data obtained from at least three different heating rates. Isoconversional methods can determine E without the knowledge or assumption of kinetic model and, unlike model-fitting approach, can reveal the dependence of E on α. The dependence of E on α is considered as reliable criterion of the process complexity [13,14]. If E does not depend on α, the investigated process is simple and can be described by unique kinetic triplet. If E depends on α, the process is complex and the shape of the curve E vs. α indicates the possible reaction mechanism [13–15]. It is suggested that dependence of E on α should be investigated by isoconversional methods prior to calculation of the kinetic parameters by any method [14]. On the other hand, isoconversional methods do not give any information about A and $f(\alpha)$. Therefore, in this article the kinetic analysis of the non-isothermal degradation of pure PHB and PHB/25A nanocomposites is performed according to algorithm proposed by Budrugeac [15]. The application of this algorithm begins with isoconversional methods in order to establish the dependence of E on α. It was

* Corresponding author. Tel.: +385 21 329 459; fax: +385 21 329 461.
E-mail address: merceg@ktf-split.hr (M. Erceg).

0040-6031/$ – see front matter © 2008 Elsevier B.V. All rights reserved.
doi:10.1016/j.tca.2008.07.009

Table 1
Characteristics of Cloisite25A

Name	Cloisite25A
Organic modifier concentration	95 mmol/100 g clay
Moisture (%)	<2%
Weight loss on ignition (%)	34
Density (g cm^{-3})	1.87
Typical dry particle size	
<2 μm	10%
<6 μm	50%
<13 μm	90%

shown that in cases when E does not depend on α, the invariant kinetic parameters (IKP) method associated with the criterion of the independence of kinetic parameters on the heating rate (Pérez-Maqueda et al. criterion [16]) is recommended for evaluation of the kinetic triplet without any assumptions concerning kinetic model.

2. Experimental

2.1. Materials

Poly(3-hydroxybutyrate) (PHB), kindly supplied by Biomer (Krailling, Germany), was used as received. Weight-average molecular weight ($\overline{M_w}$) of 350,000 g mol^{-1} was determined viscosimetrically using the equation $[\eta] = 1.18 \times 10^{-4}\overline{M_w}^{0.78}$ (chloroform, 30 °C) [17].

Organically modified montmorillonite Cloisite25A (25A) was purchased from Southern Clay Products Inc. (Gonzales, USA) and used as received. Cloisite25A is a natural montmorillonite modified with quaternary ammonium salt whose characteristics are shown in Table 1 according to the data provided by the supplier [18]. Fig. 1 shows the chemical structure of organic modifier.

2.2. Sample preparation

PHB/25A nanocomposites (100/0, 100/1, 100/3, 100/5, 100/7 and 100/10 by weight) were prepared by the solution-intercalation method. Different amounts of Cloisite25A, depending on sample composition, were dispersed in 50 mL of chloroform by vigorous mechanical stirring for 1 h and ultra-sonication at 160 W at room temperature for 30 min (pulse mode). In the each obtained dispersion 50 mL of 1% (w/v) solution of PHB in chloroform was added and then mixing and ultra-sonication were applied. Mixtures were cast on Petri dishes and the films were obtained by evaporating the solvent at room temperature and drying in vacuum at 40 °C for 24 h.

2.3. Thermal degradation

The thermal degradation of PHB/25A samples (sample mass 3.9 ± 0.6 mg) was investigated by the non-isothermal thermogravimetry (TG). TG analysis was carried out in the temperature range from 50 to 500 °C using a PerkinElmer TGS-2 system with Model 3600 Data Station. The nitrogen flow rate was 30 cm^3 min^{-1} and the heating rates were 2.5, 5, 10 and 20 °C min^{-1}. Before operating, the system was stabilised for 1 h.

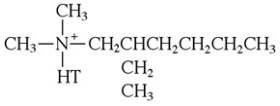

Fig. 1. Chemical structure of organic modifier. HT is hydrogenated tallow (~65% C18; ~30% C16; ~5% C14; anion: methyl sulfate).

3. Theory

The results of the non-isothermal thermogravimetry (TG) can be used to calculate the kinetic parameters of the investigated process, i.e. the activation energy (E), the pre-exponential factor (A) and kinetic model ($f(\alpha)$) which are called the "kinetic triplet". Kinetic analysis of the solid-state reactions that are ruled by a single process, the reaction rate can be expressed by Eq. (1):

$$\frac{d\alpha}{dt} \cong \beta\frac{d\alpha}{dT} = A\exp\left(\frac{E}{RT}\right)f(\alpha) \quad (1)$$

where α is the degree of conversion, β the linear heating rate (°C min^{-1}), T the absolute temperature (K), R the general gas constant (J mol^{-1} K^{-1}) and t is the time.

In this work isoconversional Flynn-Wall-Ozawa (FWO) [19,20], Kissinger-Akahira-Sunose (KAS) [21,22] and Friedman (FR) [23] methods in combination with the invariant kinetic parameters (IKP) [24] method were used to calculate the kinetic parameters of the non-isothermal degradation of PHB and PHB/25A nanocomposites in accordance with the algorithm suggested by Budrugeac [15] which enables the calculation of true values of E and A as well as the determination of empirical kinetic models $f(\alpha)$, without any assumptions concerning kinetic model.

3.1. Isoconversional methods

Isoconversional methods enable determination of E directly from experimental $\alpha - T$ data ($\alpha = (m_0 - m)/(m_0 - m_f)$, where m_0, m and m_f refer to the initial, actual and residual mass of the sample) obtained at several heating rates without the knowledge of $f(\alpha)$. Furthermore, these methods allow the dependence of E on α to be obtained.

Flynn-Wall-Ozawa (FWO) method is a linear integral method based on Eq. (2):

$$\log\beta = \log\frac{AE}{Rg(\alpha)} - 2.315 - 0.4567\frac{E}{RT} \quad (2)$$

Kissinger-Akahira-Sunose (KAS) is a linear integral method based on Eq. (3):

$$\ln\frac{\beta}{T^2} = \ln\frac{AR}{Eg(\alpha)} - \frac{E}{RT} \quad (3)$$

Friedman (FR) method is a linear differential method based on Eq. (4):

$$\ln\left[\beta\frac{d\alpha}{dT}\right] = \ln A + \ln f(\alpha) - \frac{E}{RT} \quad (4)$$

For α = const., the plots $\log\beta$ vs. $1/T$, $\ln(\beta/T^2)$ vs. $1/T$ and $\ln[\beta\, d\alpha/dT]$ vs. $1/T$ obtained from $\alpha - T$ curves recorded at several heating rates should be straight lines whose slope allows calculation of E by means of FWO, KAS and FR method, respectively.

Invariant kinetic parameters (IKP) method requires several $\alpha - T$ curves recorded at different heating rates. IKP method gives values of the invariant kinetic parameters, E_{inv} and A_{inv}, which correspond to the true kinetic model that describes the investigated process at all heating rates [25]. It is based on the existence of the linear compensation effect (Eq. (5)) between E and $\ln A$ obtained for the same TG curve by various theoretical kinetic models:

$$\ln A = a^* + b^*E \quad (5)$$

where a^* and b^* are the compensation effect parameters.

These values of E and $\ln A$ are obtained by using the Coats-Redfern (CR) method [26] (Eq. (6))

$$\ln\frac{g(\alpha)}{T^2} \cong \ln\frac{AR}{\beta E} - \frac{E}{RT} \quad (6)$$

Table 2
Algebraic expressions for $f(\alpha)$ and $g(\alpha)$ for the most frequently used mechanisms [25,27]

Mechanism	Symbol	$f(\alpha)$	$g(\alpha)$
Reaction order model	Fn[a]	$(1-\alpha)^m$	$-\ln(1-\alpha)$, for $n=1$ $(1-(1-\alpha)^{(-n+1)})/(-n+1)$, for $n \neq 1$
Random nucleation and growth of nuclei (Avrami-Erofeev eq.)	Am[b] ($0.5 \leq m \leq 4$)	$m(1-\alpha)[-\ln(1-\alpha)]^{(1-(1/m))}$	$[-\ln(1-\alpha)]^{1/m}$
1D diffusion (parabolic law)	D1	$1/2\alpha$	α^2
1D diffusion (bidimensional particle shape)	D2	$1/[-\ln(1-\alpha)]$	$(1-\alpha)\ln(1-\alpha)+\alpha$
1D diffusion (tridimensional particle shape) (Jander eq.)	D3	$(3(1-\alpha)^{2/3})/(2[1-(1-\alpha)^{1/3}])$	$[1-(1-\alpha)^{1/3}]^2$
1D diffusion (tridimensional particle shape) (Ginstling Brounshtein eq.)	D4	$3/(2[(1-\alpha)^{-1/3}-1])$	$(1-2\alpha/3)-(1-\alpha)^{2/3}$
Power law	Pz	$z\alpha^{[1-(1/z)]}$	$\alpha^{1/z}$
Prout-Tomkins	PT	$\alpha(1-\alpha)$	$\ln(\alpha/1-\alpha)$

[a] $n=1/2$ corresponds to phase boundary controlled reaction (contracting area) and $n=2/3$ corresponds to phase boundary controlled reaction (contracting volume).
[b] $m=1$, 2, 3 or 4 when the growth rate of nuclei is proportional to the interphase area and can be 0.5; 1.5 or 2.5 in some cases of diffusion controlled growth rate of nuclei.

$$g(\alpha) = \int_0^{\alpha} \frac{1}{f(a)}\,\mathrm{d}\alpha \tag{7}$$

for each theoretical kinetic model, $g(\alpha)$, and each heating rate, β, from the slope and intercept of plots $\ln[g(\alpha)/T^2]$ vs. $1/T$. Algebraic expressions for the most frequently used mechanisms are shown in Table 2.

If the compensation effect exists, the straight lines $\ln A$ vs. E should be obtained for each heating rate and should intersect in a point that corresponds to the true values of E and $\ln A$ for the true kinetic model, which were called by Lesnikovich and Levchik the invariant kinetic parameters, E_{inv} and A_{inv} [24]. Due to the fact that certain variations of the experimental condition determine region of intersection, the intersection is only approximate.

Therefore, in order to eliminate the influence of experimental conditions on determination of E_{inv} and A_{inv}, they are determined from the slope and intercept of the supercorellation relation (Eq. (8)):

$$a^* = \ln A_{inv} - b^* E_{inv} \tag{8}$$

IKP method can be used only if the E does not depend on α, what must be previously checked by isoconversional methods. Than, IKP method can be used for the numerical evaluation of $f_{inv}(\alpha)$, by introducing values of the invariant kinetic parameters E_{inv} and A_{inv} in Eq. (1) [28]. The shape of experimental curves $f_{inv}(\alpha)$ vs. α suggests the algebraic expression of $f(\alpha)$ corresponding to analysed process. The correctness of kinetic analysis is checked by criterion suggested by Pérez-Maqueda et al. [16]. This criterion states that only in the case of true $f(\alpha)$ all experimental data (at all heating rates) lie on the single straight line $\ln[(\mathrm{d}\alpha/\mathrm{d}t)/f(\alpha)]$ vs. $1/T$ whose slope and intercept give the true values of the activation energy and pre-exponential factor. When the experimental results $\ln[(\mathrm{d}\alpha/\mathrm{d}t)/f(\alpha)]$ vs. $1/T$ are spread in separate lines for each heating rate then considered $f(\alpha)$ does not fulfil this criterion, i.e. it is not capable to fit experimental results.

4. Results and discussion

It was shown in our previous study [7] that PHB/25A nanocomposites with intercalated morphology were formed. Differential scanning calorimetry (DSC) analysis showed that Cloisite25A acted as a nucleating agent and increased the crystallization rate of PHB. At the same time due to intercalation of PHB chains into Cloisite25A layers overall degree of crystallinity of PHB decreased. TG analysis showed that the addition of Cloisite25A improved the thermal stability of PHB in all investigated amounts and the most pronounced effect had addition of 5 wt.% [7].

The aim of this work is to perform kinetic analysis of the non-isothermal degradation of pure PHB and PHB/25A nanocomposites. The experimental data for the kinetic analysis were obtained from the non-isothermal thermogravimetry. The thermogravimetric (TG) curves for pure PHB and PHB/25A nanocomposites at the heating rate of 2.5 °C min^{-1} are shown in Fig. 2.

Kinetic analysis is described on a sample PHB/25A 100/5, while the results for other samples are shown in corresponding tables and figures. The non-isothermal degradation of PHB and PHB/25A nanocomposites is a solid-state process. Solid-state processes can be simple or very complex. Therefore, one should first establish the complexity of the process, i.e. dependence of E on α. In order to evaluate the dependence of E on α for the non-isothermal degradation of pure PHB and PHB/25A nanocomposites, FWO, KAS and FR methods were used. For selected α = const., the plots $\log\beta$ vs. $1/T$, $\ln(\beta/T^2)$ vs. $1/T$ and $\ln[\beta\,\mathrm{d}\alpha/\mathrm{d}T]$ vs. $1/T$ are obtained and from their slopes values of E are calculated by means of FWO, KAS and FR method, respectively. The dependences of E on α evaluated by means of FWO (a), KAS (b) and FR (c) method are shown in Fig. 3 (a–c), respectively. The average values of E in the conversion range in which E values are practically constant are shown in Table 3.

E is practically independent on α for all investigated samples in a very wide conversion range. This means that from the kinetical point of view investigated process is simple (one-step process) and can be described by unique kinetic triplet.

This is in an agreement with the well-known fact that thermal degradation of PHB proceeds exclusively by a one step, random chain scission reaction (β-elimination) [29]. Based on these results, it can be assumed that the non-isothermal degradation of PHB/25A

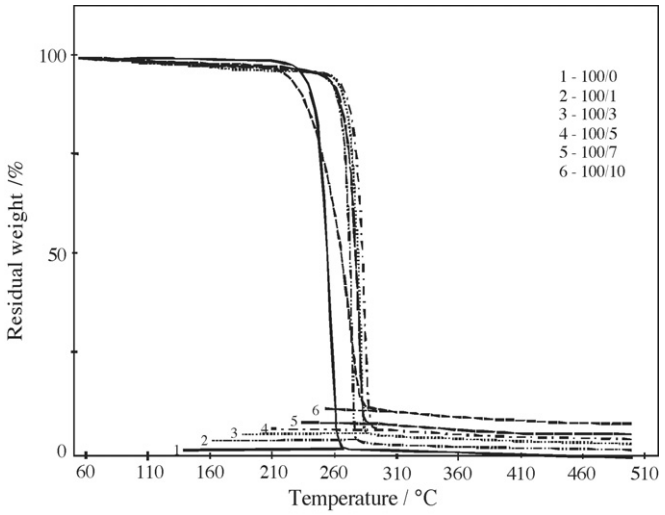

Fig. 2. TG curves of the non-isothermal degradation of pure PHB and PHB/25A nanocomposites at the heating rate of 2.5 °C min^{-1}.

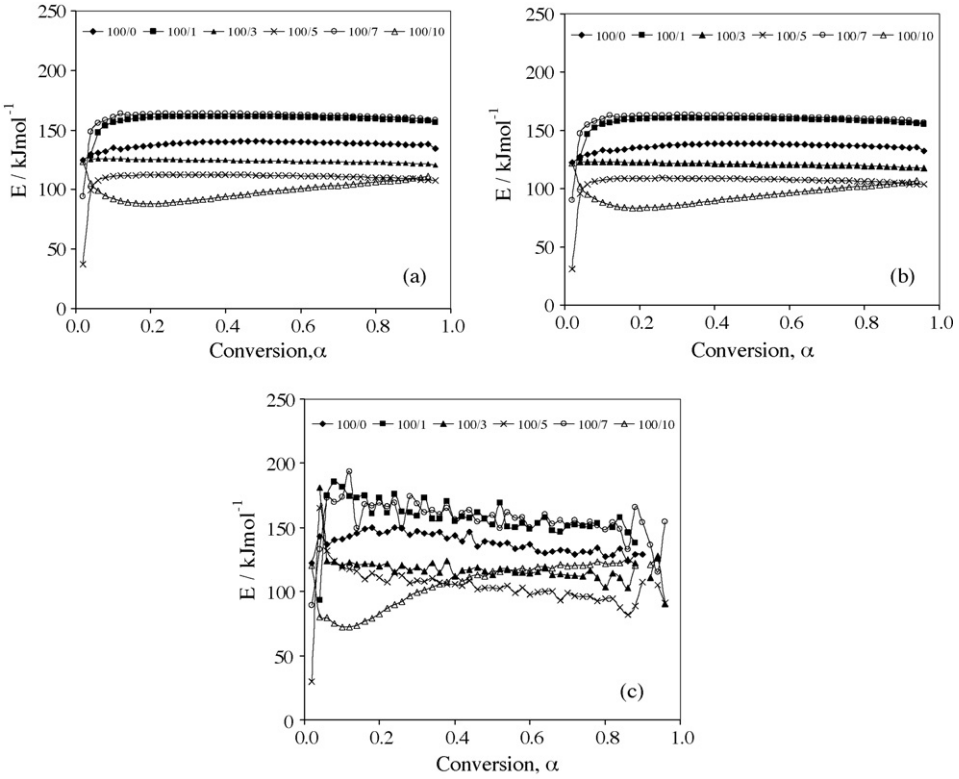

Fig. 3. The dependence of E on α evaluated by means of FWO (a), KAS (b) and FR (c) method for the non-isothermal degradation of pure PHB and PHB/25A nanocomposites.

nanocomposites proceeds also by one step process since in the very wide conversion range E is practically constant.

Furthermore, in this case IKP can be used for evaluation of true kinetic triplet. The evaluation of the values of E and $\ln A$ needed for IKP method was performed by using CR method. Using the relation of the compensation effect (Eq. (5)) the existence of the compensation effect between values of E and $\ln A$ obtained by CR method is checked. Fig. 4(a) shows the compensation relationship for the non-isothermal degradation of PHB/25A 100/5 nanocomposite.

From their slopes and intercepts the so called compensation parameters a^* and b^* are obtained for each heating rate. For calculation of a^* and b^*, we have used values of E and $\ln A$ only from those $g(\alpha)$ that show correlation coefficient $r^2 > 0.99$ at all heating rates. Furthermore, these lines intersect in a very small region (Fig. 4(b)) what indicates that the non-isothermal degradation of PHB/25A 100/5 nanocomposite is really one-step process. Since the intersection of these lines is dependent on experimental conditions and therefore approximate, the calculation of the invariant kinetic parameters, E_{inv} and A_{inv} is performed using the supercorrelation relation (Eq. (8)). The results from Fig. 5 show that, in case of PHB/25A 100/5 nanocomposite, between compensation parameters a^* and b^* exists supercorrelation relation since straight lines are obtained, and from the slope and intercept E_{inv} and A_{inv} are obtained, respectively.

In the same way, the existence of the compensation effect between E and $\ln A$ and one step-process are confirmed as well as the calculation of E_{inv} and A_{inv} for all other investigated samples is performed. Calculated values of E_{inv} and A_{inv} for pure PHB and PHB/25A nanocomposites are shown in Table 4.

Obtained values of E_{inv} are in a good agreement with E values obtained by isoconversional methods, especially by Friedman method. Similar behaviour has already been observed for other polymers and polymeric materials [15,25]. Values of E_{inv} and A_{inv} allow numerical determination of $f_{inv}(\alpha)$ by introducing them into

Table 3
The average values of E obtained by isoconversional of FWO, KAS and FR methods

	PHB/25A					
	100/0 $0.10 \le \alpha \le 0.90$[a]	100/1 $0.10 \le \alpha \le 0.90$[a]	100/3 $0.10 \le \alpha \le 0.90$[a]	100/5 $0.10 \le \alpha \le 0.90$[a]	100/7 $0.10 \le \alpha \le 0.90$[a]	100/10 $0.40 \le \alpha \le 0.90$[a]
FWO						
E (kJ mol^{-1})	138.8 ± 1.7	160.5 ± 1.1	124.3 ± 0.9	111.8 ± 0.8	162.9 ± 1.0	102.0 ± 4.5
r^2	0.99984	0.99993	0.99986	0.99920	0.99989	0.99934
KAS						
E (kJ mol^{-1})	137.1 ± 1.7	159.6 ± 1.1	121.3 ± 1.0	108.2 ± 0.8	162.0 ± 1.1	97.9 ± 4.6
r^2	0.99986	0.99994	0.99994	0.99901	0.99990	0.99928
FR						
E (kJ mol^{-1})	139.2 ± 7.1	159.7 ± 9.5	116.6 ± 4.2	104.7 ± 6.7	160.4 ± 9.2	118.0 ± 4.2
r^2	0.99841	0.99925	0.99953	0.99433	0.99904	0.99815

[a] Conversion, α.

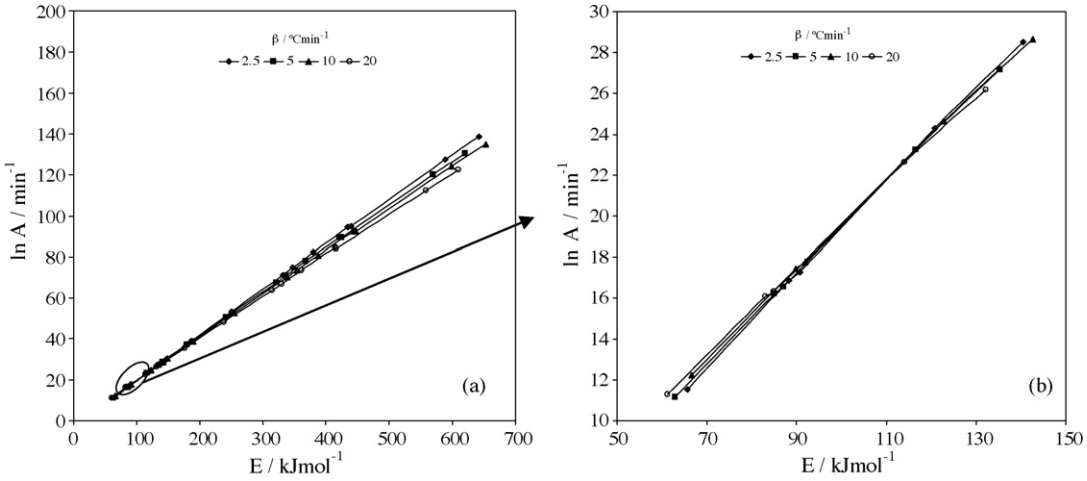

Fig. 4. The compensation relationship (a) and the enlarged region of interception (b) for the PHB/25A 100/5 nanocomposite.

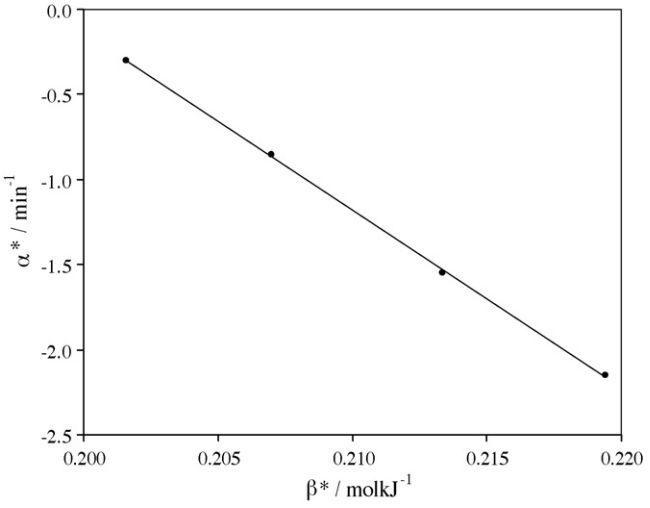

Fig. 5. The supercorrelation relationship for PHB/25A 100/5 nanocomposite.

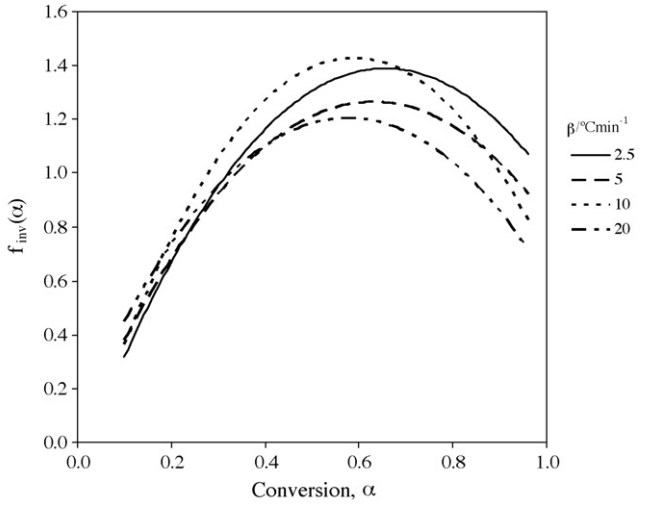

Fig. 6. The experimental dependence of $f_{inv}(\alpha)$ vs. α for PHB/25A 100/5 nanocomposite.

Eq. (1). Fig. 6 shows the curves $f_{inv}(\alpha)$ vs. α for the sample PHB/25A 100/5. The curves exhibit the maximum as well as for all other samples considered in this work.

These curves are compared with the curves $f(\alpha)$ vs. α of the theoretical kinetic models of which only Avrami-Erofeev kinetic models and Prout-Tomkins autocatalytic model (Table 2) exhibit maximum. It s well known that the true kinetic model should give the value of E similar to those obtained by isoconversional methods. By using Coats-Redfern method Prout-Tomkins kinetic model gives the average value of $E = 488\ kJ\ mol^{-1}$ at four heating rates, while Avrami-Erofeev kinetic models A2 and A2,5 give average values of $E = 144\ kJ\ mol^{-1}$ and $E = 119\ kJ\ mol^{-1}$ for PHB/25A 100/5, respectively. Average value obtained by isoconversional FWO, KAS and FR methods is $E = 138\ kJ\ mol^{-1}$ (Table 3). This suggests that the non-isothermal degradation of pure PHB and PHB/25A nanocomposites occurs through mechanism like those represented by the Avrami-Erofeev equations, rather than Prout-Tomkins equation.

However, as expected, any theoretical Avrami-Erofeev kinetic model (Eq. (9)) cannot fit exactly the experimental $f_{inv}(\alpha)$ vs. α curve:

$$f(\alpha) = m(1-\alpha)[-\ln(1-\alpha)]^p \quad (9)$$

Therefore, it was necessary to calculate the empirical kinetic models that will fit exactly the experimental $f_{inv}(\alpha)$ vs. α curve, i.e. it

Table 4
Values of invariant kinetic parameters for pure PHB and PHB/25A nanocomposites

	PHB/25A					
	100/0 $0.10 \le \alpha \le 0.90$[a]	100/1 $0.10 \le \alpha \le 0.90$[a]	100/3 $0.10 \le \alpha \le 0.90$[a]	100/5 $0.10 \le \alpha \le 0.90$[a]	100/7 $0.10 \le \alpha \le 0.90$[a]	100/10 $0.40 \le \alpha \le 0.90$[a]
E_{inv} (kJ mol^{-1})	140.0	161.6	115.9	105.7	160.3	115.4
$\ln A_{inv}$ (min^{-1})	29.8884	33.7624	23.2090	21.0374	32.9536	22.7677
r^2	0.99950	0.99980	0.99998	0.99486	0.99650	0.99889

[a] Conversion, α.

Table 5
The parameters m and p of empirical kinetic models for pure PHB and PHB/25A nanocomposites

β (°C min^{-1})	PHB/25A 100/0			PHB/25A 100/1		
	m	p	r^2	m	p	r^2
2.5	2.57	0.63	0.99021	4.12	1.01	0.99705
5	2.72	0.63	0.99275	4.10	0.98	0.99553
10	2.52	0.56	0.99242	3.82	0.92	0.99688
20	2.42	0.52	0.98789	3.73	0.88	0.99278
Average value	2.56	0.58	0.99082	3.94	0.95	0.99556
β (°C min^{-1})	PHB/25A 100/3			PHB/25A 100/5		
	m	p	r^2	m	p	r^2
2.5	3.89	0.98	0.99525	3.86	1.03	0.99723
5	3.88	0.98	0.99685	3.50	0.95	0.99705
10	3.82	0.94	0.99764	3.94	0.96	0.99850
20	3.78	0.92	0.99767	3.29	0.86	0.99789
Average value	3.84	0.95	0.99685	3.65	0.95	0.99767
β (°C min^{-1})	PHB/25A 100/7			PHB/25A 100/10		
	m	p	r^2	m	p	r^2
2.5	3.28	0.80	0.99616	3.11	0.74	0.98962
5	3.29	0.77	0.99569	2.91	0.76	0.99791
10	3.14	0.73	0.99597	3.08	0.83	0.99494
20	3.10	0.70	0.99228	3.23	0.90	0.99670
Average value	3.20	0.75	0.99502	3.08	0.81	0.99479

was necessary to calculate the parameters m and p of the empirical kinetic models. The parameters m and p are calculated for each heating rate from the intercepts and slopes of plots Y vs. $\ln[-\ln(1-\alpha)]$ (Eq. (11)):

$$Y \equiv \ln \frac{d\alpha/dt}{1-\alpha} - \ln A_{inv} + \frac{E_{inv}}{RT} = \ln m + p \ln[-\ln(1-\alpha)] \quad (11)$$

obtained by introducing Eq. (9) into Eq. (1). If $p = 1 - 1/m$, then empirical $f(\alpha)$ corresponds to the theoretical Avrami-Erofeev kinetic model. Values of the parameters m and p of empirical kinetic models for pure PHB and PHB/25A nanocomposites are shown in Table 5.

The criterion by Pérez-Maqueda et al. was applied on the calculated empirical kinetic models (average values were considered). This criterion states that only in the case of true kinetic model all experimental results, at all heating rates, lie on the single straight line whose slope and intercept give the true values of the E and $\ln A$ (Fig. 7). Calculated empirical kinetic models fulfil this criterion since straight lines are obtained for all investigated samples ($r^2 > 0.99$, Table 6) and from their slopes and intercepts the true values of E and $\ln A$ are obtained (Table 6). These values of activation energy are in a very good agreement with the values obtained by isoconversional methods.

All considered theoretical kinetic models from Table 2 do not fulfil Pérez-Maqueda et al. criterion since the calculated data are spread in different lines.

To check the correctness of the kinetic analysis, $d\alpha/dt$ data calculated using Eq. (1) and kinetic parameters from Table 6, were compared to experimental ones. Fig. 8(a) and (b) shows comparison of calculated and experimental $d\alpha/dt$ data for pure PHB and PHB/25A 100/5 nanocomposite. The results show good agreement between calculated and experimental data with very low values of the standard deviations (S.D.).

Finally, the true values of E and $\ln A$ allow us to calculate the rate constant, k of the non-isothermal degradation for pure PHB and PHB/25A nanocomposites (Fig. 9). The addition of Cloisite25A reduces the rate constant compared to pure PHB, i.e. the rate of

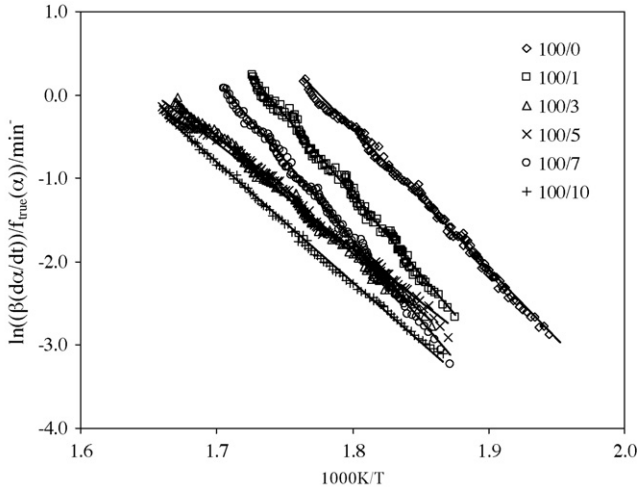

Fig. 7. Application of the Pérez-Maqueda et al. criterion on the empirical kinetic models.

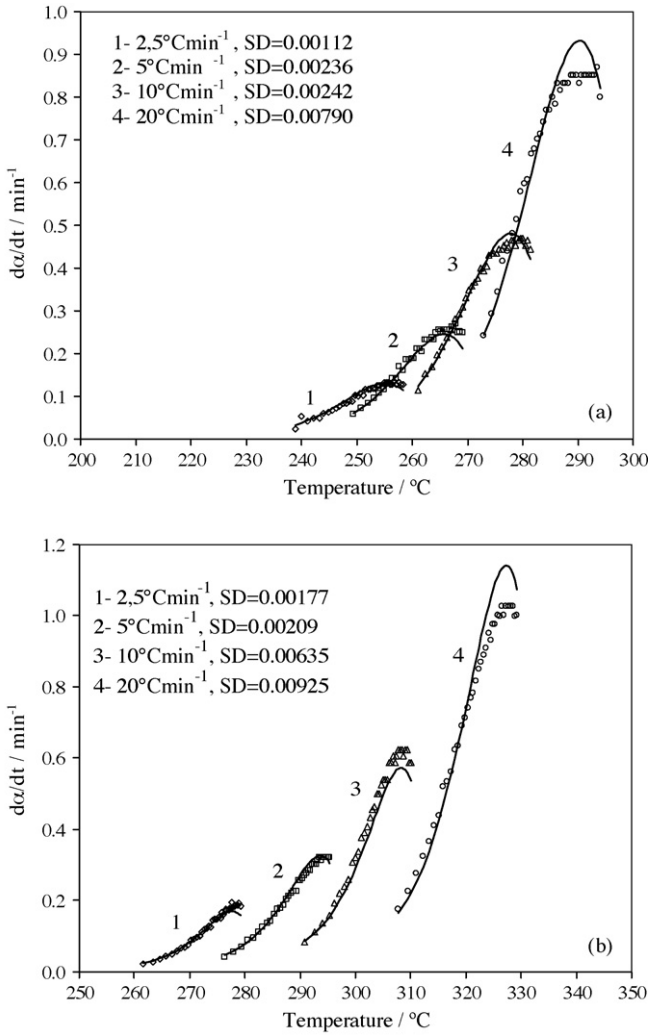

Fig. 8. Experimental (points) and calculated $d\alpha/dt$ data (lines) for pure PHB (a) and PHB/25A 100/5 nanocomposite.

Table 6
True values of E and $\ln A$ corresponding to the calculated empirical kinetic models

PHB/25A	Conversion, α	$f(\alpha)$	E (kJ mol^{-1})	$\ln A$ (min^{-1})	r^2
100/0	$0.10 \le \alpha \le 0.90$	$2.56\,(1-\alpha)[-\ln(1-\alpha)]^{0.58}$	139.2	29.7235	0.99540
100/1	$0.10 \le \alpha \le 0.90$	$3.94\,(1-\alpha)[-\ln(1-\alpha)]^{0.95}$	159.9	33.3906	0.99387
100/3	$0.10 \le \alpha \le 0.90$	$3.84\,(1-\alpha)[-\ln(1-\alpha)]^{0.95}$	116.7	23.3644	0.99665
100/5	$0.10 \le \alpha \le 0.90$	$3.65\,(1-\alpha)[-\ln(1-\alpha)]^{0.95}$	105.6	21.0127	0.99084
100/7	$0.10 \le \alpha \le 0.90$	$3.20\,(1-\alpha)[-\ln(1-\alpha)]^{0.75}$	160.0	32.8901	0.99650
100/10	$0.40 \le \alpha \le 0.90$	$3.08\,(1-\alpha)[-\ln(1-\alpha)]^{0.81}$	118.3	23.3757	0.99738

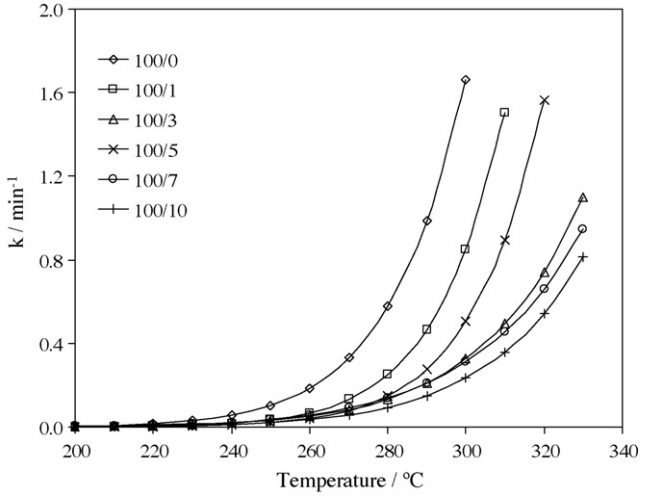

Fig. 9. Dependence of k on T for pure PHB and PHB/25A nanocomposites.

the non-isothermal degradation of PHB. This is probably due to the fact that layered silicates act as mass transport barrier into and out of the degradation zone. The lowest rate constant shows PHB/25A 100/10 nanocomposite what is probably due to, beside above mentioned effects, the more pronounced char formation at this higher Cloisite25A loading [7].

5. Conclusions

PHB/25A nanocomposites were prepared by the solution-intercalation method. Isoconversional Flynn-Wall-Ozawa, Kissinger-Akahira-Sunose and Friedman methods in combination with invariant kinetic parameters method were used for the kinetic analysis of the non-isothermal degradation of pure PHB and PHB/25A nanocomposites. The use of IKP method led to the invariant kinetic parameters which allowed numerical determination of kinetic model, $f_{inv}(\alpha)$. The shape of the curves $f_{inv}(\alpha)$ vs. α suggested that investigated process can be kinetically described by Avrami-Erofeev equation, $f(\alpha) = m(1-\alpha)[-\ln(1-\alpha)]^p$, and the parameters m and p, i.e. empirical $f(\alpha)$ were evaluated for each sample. Empirical $f(\alpha)$ fulfilled Pérez-Maqueda et al. criterion. E values corresponding to empirical $f(\alpha)$ are in a very good agreement with the E values obtained by isoconversional methods. Also, calculated $d\alpha/dt$ vs. T curves fit excellently experimental $d\alpha/dt$ vs. T curves what indicates that the true kinetic triplets of the investigated process are obtained. The addition of Cloisite25A reduces the rate of the non-isothermal degradation of PHB.

Acknowledgements

The represented results emerged from the scientific project (polymer blends with biodegradable components) financially supported by the Ministry of Science, Education and Sports of the Republic of Croatia.

References

[1] E.G. Fernandes, M. Pietrini, E. Chiellini, Macrom. Symp. 218 (2004) 157–164.
[2] A. El Hadi, R. Schnabel, E. Straube, G. Müller, S. Henning, Polym. Testing 21 (2002) 665–674.
[3] R.C. Baltieri, L.H.I. Mei, J. Bartoli, Macrom. Symp. 197 (2003) 33–44.
[4] S.A. Jose, S. Aprem, B. Francis, M.C. Chandy, P. Werner, A. Alstaedt, S. Thomas, Eur. Polym. J. 40 (2004) 2105–2115.
[5] D.N. Bikiaris, G.Z. Papageorgiou, E. Pavlidou, N. Vouroutzis, P. Palatzoglou, G.P. Karayannidis, J. Appl. Polym. Sci. 100 (2006) 2684–2696.
[6] J. Brandrup, E.H. Immergut, E.A. Grulke, Polymer Handbook, vol. 1, 4th ed., John Wiley & Sons, New Jersey, 1999, p. V/26.
[7] M. Erceg, Modification of properties of biodegradable poly(3-hydroxybutyrate), PhD Thesis, University of Split, 2007.
[8] C. Chen, B. Fei, S. Peng, Y. Zhuang, L. Dong, Z. Feng, J. Appl. Polym. Sci. 84 (2002) 1789–1796.
[9] M.Y. Lee, T.S. Lee, W.H. Park, Macromol. Chem. Phys. 202 (2001) 1257–1261.
[10] S. Li, J. He, P.H. Yu, M.K. Cheung, J. Appl. Polym. Sci. 89 (2003) 1530–1536.
[11] S. Vyazovkin, C.A. Wight, Thermochim. Acta 340/341 (1999) 53–68.
[12] M. Maciejewski, Thermochim. Acta 355 (2000) 145–154.
[13] S. Vyazovkin, A.I. Lesnikovich, Thermochim. Acta 165 (1990) 273–280.
[14] S. Vyazovkin, N. Sbirrazzuoli, Macromol. Rapid Commun. 27 (2006) 1515–1532.
[15] P. Budrugeac, Polym. Degrad. Stab. 89 (2005) 265–273.
[16] L.A. Pérez-Maqueda, J.M. Criado, F.J. Gotor, J. Malek, J. Phys. Chem. A 106 (2002) 2862–2868.
[17] S. Akita, Y. Einaga, Y. Miyaki, H. Fujita, Macromolecules 9 (1976) 774–780.
[18] http://www.scprod.com/product_bulletins/PB%20Cloisite%2025A.pdf (accessed on 10.06.2008).
[19] J.H. Flynn, L.A. Wall, J. Res. Natl. Bur. Stand. 70A (1966) 487–523.
[20] T. Ozawa, Bull. Chem. Soc. Jpn. 38 (1965) 1881–1889.
[21] H.E. Kissinger, Anal. Chem. 29 (1957) 1702–1706.
[22] T. Akahira, T. Sunose, Res. Report Chiba Inst. Technol. 16 (1971) 22–31.
[23] H.L. Friedman, J. Polym. Sci. 6C (1963) 183–195.
[24] A.I. Lesnikovich, S.V. Levchik, J. Therm. Anal. 27 (1983) 89–94.
[25] P. Budrugeac, E. Segal, Int. J. Chem. Kin. 33 (2001) 564–573.
[26] A.W. Coats, J.P. Redfern, Nature 201 (1964) 68–69.
[27] K. Pielichowski, J. Njuguna, Thermal Degradation of Polymeric Materials, Rapra Technology Limited, Shawbury, 2005, p. 40.
[28] P. Budrugeac, E. Segal, L.A. Pérez-Maqueda, J.M. Criado, Polym. Degrad. Stab. 84 (2004) 311–320.
[29] N. Grassie, E.J. Murray, Polym. Degrad. Stab. 6 (1984) 127–134.